





Article

New arsenate minerals from the Arsenatnaya fumarole, Tolbachik volcano, Kamchatka, Russia. XIX. Axelite, $\text{Na}_{14}\text{Cu}_7(\text{AsO}_4)_8\text{F}_2\text{Cl}_2$

Igor V. Pekov^{1*}, Natalia V. Zubkova¹, Atali A. Agakhanov², Vasily O. Yapaskurt¹, Dmitry I. Belakovskiy², Sergey N. Britvin³ , Evgeny G. Sidorov^{4,†}, Anton V. Kutyrev⁴  and Dmitry Yu. Pushcharovskiy¹

¹Faculty of Geology, Moscow State University, Vorobiev Gory, 119991 Moscow, Russia; ²Fersman Mineralogical Museum of the Russian Academy of Sciences, Leninsky Prospekt 18-2, 119071 Moscow, Russia; ³Dept. of Crystallography, St Petersburg State University, University Embankment 7/9, 199034 St Petersburg, Russia; and ⁴Institute of Volcanology and Seismology, Far Eastern Branch of Russian Academy of Sciences, Piip Boulevard 9, 683006 Petropavlovsk-Kamchatsky, Russia

Abstract

The new mineral axelite, ideally $\text{Na}_{14}\text{Cu}_7(\text{AsO}_4)_8\text{F}_2\text{Cl}_2$, was found in the Arsenatnaya fumarole at the Second scoria cone of the Northern Breakthrough of the Great Tolbachik Fissure Eruption, Tolbachik volcano, Kamchatka, Russia. It is associated with sylvite, halite, arsmirandite, bradaczekite, johillerite, tilasite, ericlxmanite, lammerite, hematite, tenorite, cassiterite, pseudobrookite, apththitalite-group sulfates, anhydrite, fluoborite, sanidine and fluorophlogopite. Axelite occurs as tabular, quadratic, rectangular or stronger distorted crystals up to $0.02 \times 0.1 \times 0.1$ mm, sometimes combined in interrupted crusts up to 0.4 mm across overgrowing sylvite. It is transparent, sky-blue, with vitreous lustre. Cleavage was not observed. D_{calc} is 3.662 g cm^{-3} . Axelite is optically uniaxial (–), $\epsilon = 1.650(4)$ and $\omega = 1.678(4)$. Chemical composition (wt.%, electron microprobe data) is: Na₂O 22.54, K₂O 0.08, CaO 0.04, MgO 0.05, CuO 26.69, P₂O₅ 1.75, V₂O₅ 0.15, As₂O₅ 44.14, SO₃ 0.04, F 1.57, Cl 3.60, –O=(F,Cl) –1.47, total 99.18. The empirical formula based on O+F+Cl=36 apfu is $\text{Na}_{14.37}\text{K}_{0.03}\text{Ca}_{0.01}\text{Mg}_{0.02}\text{Cu}_{6.63}\text{P}_{0.49}\text{V}_{0.03}\text{As}_{7.59}\text{S}_{0.01}\text{O}_{32.36}\text{F}_{1.63}\text{Cl}_{2.01}$. Axelite is tetragonal, $P4bm$, $a = 14.5957(2)$, $c = 8.34370(18)$ Å, $V = 1777.51(6)$ Å³ and $Z = 2$. The strongest reflections of the powder X-ray diffraction (XRD) pattern [$d, \text{Å}(I)(hkl)$] are: 8.32(44)(001), 5.156(47)(220), 4.168(21)(002), 3.246(34)(222), 3.180(61)(331), 2.747(100)(402), 2.709(36)(511) and 2.580(29)(440). The crystal structure, solved from single-crystal XRD data ($R = 4.50\%$), is unique. It is based on the heteropolyhedral chains built by clusters formed by CuO_4Cl square pyramids connected with AsO_4 tetrahedra. Adjacent chains are connected *via* common vertices of AsO_4 tetrahedra with CuO_4Cl pyramids to form a heteropolyhedral pseudo-framework. Axelite is remotely related, in both structural and chemical aspects, to lavendulan-like minerals and synthetic compounds. The mineral is named in honour of the outstanding Finnish–Russian crystallographer, mineralogist and material scientist Axel Gadolin (1828–1892).

Keywords: axelite, new mineral, fluoro-chloro-arsenate, sodium copper arsenate, crystal structure, lavendulan group, fumarole sublimate, Tolbachik volcano, Kamchatka

(Received 27 August 2022; accepted 26 October 2022; Accepted Manuscript published online: 21 November 2022; Associate Editor: Elena Zhitova)

Introduction

The present article continues the series of papers devoted to descriptions of new arsenates from the Arsenatnaya fumarole at the Second scoria cone of the Northern Breakthrough of the Great Tolbachik Fissure Eruption 1975–1976, Tolbachik volcano, Kamchatka Peninsula, Far-Eastern Region, Russia. Twenty one new minerals were characterised in the previous papers of the series, namely yurmarinite $\text{Na}_7(\text{Fe}^{3+}, \text{Mg}, \text{Cu})_4(\text{AsO}_4)_6$ (Pekov *et al.*, 2014a), two polymorphs of $\text{Cu}_4\text{O}(\text{AsO}_4)_2$, ericlxmanite and kozyrevskite (Pekov *et al.*, 2014b), popovite $\text{Cu}_5\text{O}_2(\text{AsO}_4)_2$ (Pekov *et al.*, 2015a), structurally related shchurovskiyite $\text{K}_2\text{CaCu}_6\text{O}_2(\text{AsO}_4)_4$ and dmisokolovite $\text{K}_3\text{Cu}_5\text{AlO}_2(\text{AsO}_4)_4$

(Pekov *et al.*, 2015b), katiarsite $\text{KTiO}(\text{AsO}_4)$ (Pekov *et al.*, 2016a), melanarsite $\text{K}_3\text{Cu}_7\text{Fe}^{3+}\text{O}_4(\text{AsO}_4)_4$ (Pekov *et al.*, 2016b), pharmazincite KZnAsO_4 (Pekov *et al.*, 2017a), arsenowagnerite $\text{Mg}_2(\text{AsO}_4)\text{F}$ (Pekov *et al.*, 2018b), arsenatotitanite $\text{NaTiO}(\text{AsO}_4)$ (Pekov *et al.*, 2019a), the two isostructural minerals edtolite $\text{K}_2\text{NaCu}_5\text{Fe}^{3+}\text{O}_2(\text{AsO}_4)_4$ and alumoedtolite $\text{K}_2\text{NaCu}_5\text{AlO}_2(\text{AsO}_4)_4$ (Pekov *et al.*, 2019b), anatolyite $\text{Na}_6(\text{Ca}, \text{Na})(\text{Mg}, \text{Fe}^{3+})_3\text{Al}(\text{AsO}_4)_6$ (Pekov *et al.*, 2019c), zubkovaite $\text{Ca}_3\text{Cu}_3(\text{AsO}_4)_4$ (Pekov *et al.*, 2019d), pansnerite $\text{K}_3\text{Na}_3\text{Fe}_6^{3+}(\text{AsO}_4)_8$ (Pekov *et al.*, 2020a), badalovite $\text{NaNaMg}(\text{MgFe}^{3+})(\text{AsO}_4)_3$ (Pekov *et al.*, 2020b), calciojohillerite $\text{NaCaMgMg}_2(\text{AsO}_4)_3$ (Pekov *et al.*, 2021a), yurgensonite $\text{K}_2\text{SnTiO}_2(\text{AsO}_4)_2$ (Pekov *et al.*, 2021b), paraberzeliite $\text{NaCaMg}_2(\text{AsO}_4)_3$ (Pekov *et al.*, 2022a) and khrenovite $\text{Na}_3\text{Fe}_2^{3+}(\text{AsO}_4)_3$ (Pekov *et al.*, 2022b).

In this paper the new mineral axelite (Cyrillic: акселит), ideally $\text{Na}_{14}\text{Cu}_7(\text{AsO}_4)_8\text{F}_2\text{Cl}_2$, is described. It is named in honour of the outstanding Finnish–Russian crystallographer, mineralogist and materials scientist, Academician of the Russian Academy of Sciences (St. Petersburg Emperor Academy of Sciences) Axel Gadolin (1828–1892).

*Author for correspondence: Igor V. Pekov, Email: igorpekov@mail.ru

†Deceased 20 March 2021

Cite this article: Pekov I.V., Zubkova N.V., Agakhanov A.A., Yapaskurt V.O., Belakovskiy D.I., Britvin S.N., Sidorov E.G., Kutyrev A.V. and Pushcharovskiy D.Y.u. (2023) New arsenate minerals from the Arsenatnaya fumarole, Tolbachik volcano, Kamchatka, Russia. XIX. Axelite, $\text{Na}_{14}\text{Cu}_7(\text{AsO}_4)_8\text{F}_2\text{Cl}_2$. *Mineralogical Magazine* 87, 109–117. <https://doi.org/10.1180/mgm.2022.120>

Both the new mineral and its name (symbol Axe) have been approved by the Commission on New Minerals, Nomenclature and Classification of the International Mineralogical Association (IMA2017-015a, Pekov *et al.*, 2017b). The holotype specimen is deposited in the systematic collection of the Fersman Mineralogical Museum of the Russian Academy of Sciences, Moscow with the catalogue number 95905.

Occurrence and general appearance

The Second scoria cone is a monogenetic volcano formed as a result of eruptive activity of the Northern Breakthrough of the Great Tolbachik Fissure Eruption in 1975. It is located 18 km SSW of the Ploskiy Tolbachik volcano (Fedotov and Markhinin, 1983). The Arsenatnaya fumarole belongs to the main fumarole field located at the summit of the Second scoria cone. This active, hot fumarole, its general mineralogical features and zonation of sublimate incrustations have been reported by Pekov *et al.* (2018a) and Shchipalkina *et al.* (2020). The mineralogy and geochemistry of the very interesting and unusual oxidising-type fumaroles of Tolbachik in general were recently reviewed (Pekov *et al.*, 2020c and references therein).

Among more than fifty arsenates known in the Arsenatnaya fumarole, axelite is one of the rarest minerals. It was found in only a few specimens. The specimen which became the holotype (sample #4673) was collected by us in July 2015 from a pocket ~1.5 m below the day surface, within the so-called polymineralic zone of the fumarole (zone IV: Shchipalkina *et al.*, 2020). The temperature measured using a chromel–alumel thermocouple in this pocket during sampling was 420°C. Axelite occurs as tabular, quadratic or, more typically, rectangular (flattened on {001} and sometimes slightly elongated along [100]) or stronger distorted crystals up to 0.02 × 0.1 × 0.1 mm. The crystals, typically with uneven surfaces, are formed by pinacoidal faces {001} and prismatic faces {100} and {110} (Figs 1 and 2). They are separate or combined in interrupted crusts up to 0.4 mm across overgrowing sylvite together with two other Na–Cu arsenates, arsmirandite $\text{Na}_{18}\text{Cu}_{12}\text{Fe}^{3+}\text{O}_8(\text{AsO}_4)_8\text{Cl}_5$ and bradaczekite $\text{NaCu}_4(\text{AsO}_4)_3$ (Fig. 1). Associated minerals also include halite, johillerite, tilasite, ericlxmanite, lammerite, hematite, tenorite, cassiterite, pseudobrookite, apthitalite-group sulfates, anhydrite, fluorborite, sanidine (As-bearing variety) and fluorophlogopite.

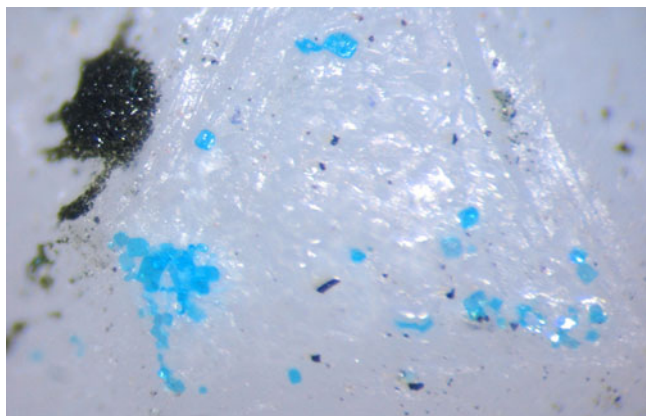


Fig. 1. Numerous sky-blue crystals and crystal clusters of axelite, dark olive-green crystal crust of arsmirandite and separate very dark blue prismatic crystals of bradaczekite on the surface of a coarse sylvite crystal. Field of view width is 2.0 mm. Sample # Tolb-4673, photo: I.V. Pekov & A.V. Kasatkin.

Axelite appears to be a ‘classic’ fumarolic mineral. We consider that it was deposited directly from hot gas as volcanic sublimate at the temperatures not lower than 420–450°C.

Physical properties and optical data

Axelite is transparent, sky-blue, with white streak and vitreous lustre. The mineral is brittle; cleavage or parting was not observed. The fracture is uneven. Density calculated using the empirical formula and unit-cell volume found from single-crystal X-ray diffraction data is 3.662 g cm⁻³.

Axelite is optically uniaxial (-), $\epsilon = 1.650(4)$, $\omega = 1.678(4)$ (589 nm). In plane-polarised light, the mineral demonstrates weak pleochroism with the following absorption scheme: E (green) > O (light green).

Chemical composition

The chemical composition of axelite was determined using a Jeol JSM-6480LV scanning electron microscope equipped with an INCA-Wave 500 wavelength-dispersive spectrometer (Laboratory of Analytical Techniques of High Spatial Resolution, Department of Petrology, Moscow State University), with an acceleration voltage of 20 kV, a beam current of 20 nA, and a 3 μm beam diameter.

The chemical data are given in Table 1. Contents of other elements with atomic numbers >6 were below detection limits. The empirical formula calculated on the basis of O+F+Cl = 36 atoms per formula unit (apfu) is $\text{Na}_{14.37}\text{K}_{0.03}\text{Ca}_{0.01}\text{Mg}_{0.02}\text{Cu}_{6.63}\text{P}_{0.49}\text{V}_{0.03}\text{As}_{7.59}\text{S}_{0.01}\text{O}_{32.36}\text{F}_{1.63}\text{Cl}_{2.01}$. The simplified formula of axelite, written taking into account the structure data (see below), is $\text{Na}_{14}(\text{Cu},\text{Na})_7[(\text{As},\text{P})\text{O}_4]_8(\text{F},\text{O})_2\text{Cl}_2$. The idealised formula is $\text{Na}_{14}\text{Cu}_7(\text{AsO}_4)_8\text{F}_2\text{Cl}_2$ which requires Na₂O 21.84, CuO 28.03, As₂O₅ 46.26, F 1.91, Cl 3.57, -O=(F,Cl) -1.61, total 100 wt.%.

X-ray crystallography and crystal structure determination details

Powder X-ray diffraction (XRD) data for axelite (Table 2) were collected with a Rigaku R-AXIS Rapid II diffractometer equipped with a cylindrical image plate detector (radius 127.4 mm) using Debye-Scherrer geometry, CoK α radiation (rotating anode with

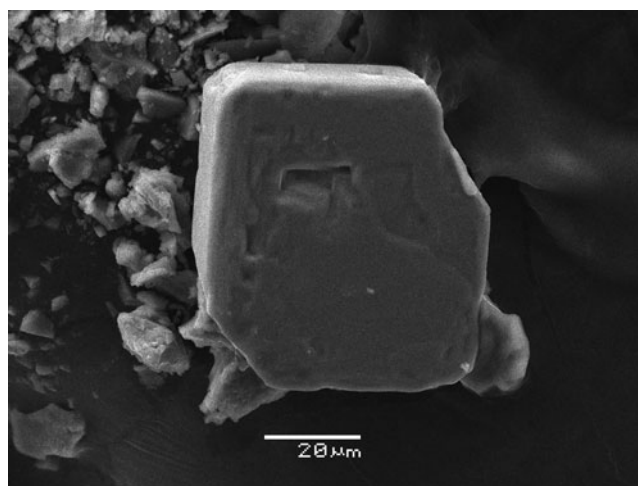


Fig. 2. Scanning electron microscopy image of a typical crystal of axelite. Sample # Tolb-4673.

Table 1. Chemical composition (wt. %) of axelite.

Constituent	Average*	Range	S.D.	Probe standard
Na ₂ O	22.54	21.75–23.45	0.70	albite
K ₂ O	0.08	0.00–0.19	0.07	orthoclase
CaO	0.04	0.00–0.14	0.04	wollastonite
MgO	0.05	0.00–0.12	0.05	diopside
CuO	26.69	25.78–27.71	0.70	Cu
P ₂ O ₅	1.75	0.87–2.53	0.59	AlPO ₄
V ₂ O ₅	0.15	0.00–0.30	0.12	Cu ₃ V ₂ S ₄
As ₂ O ₅	44.14	43.14–45.44	0.85	InAs
SO ₃	0.04	0.00–0.10	0.04	ZnS
F	1.57	1.37–1.88	0.21	fluorophlogopite
Cl	3.60	3.36–3.83	0.19	atacamite
–O = (F,Cl)	–1.47			
Total	99.18			

*Averaged for five spot analyses.

S.D. – standard deviation

Table 2. Powder X-ray diffraction data (*d* in Å) of axelite.

<i>l</i> _{obs}	<i>d</i> _{obs}	<i>l</i> _{calc} *	<i>d</i> _{calc} **	<i>h k l</i>
12	10.28	12	10.321	110
44	8.32	37	8.343	001
9	7.27	8	7.298	200
9	6.51	4, 2	6.527, 6.488	210, 111
6	5.497	3	5.493	201
47	5.156	35, 4	5.160, 5.141	220, 211
14	4.387	10	4.389	221
21	4.168	14	4.172	002
13	3.858	7	3.868	112
6	3.621	1, 1	3.642, 3.622	321, 202
9	3.341	6	3.343	401
34	3.246	3, 21	3.263, 3.244	420, 222
61	3.180	54	3.180	331
100	2.747	100	2.747	402
36	2.709	39	2.708	511
6	2.652	3	2.654	332
29	2.580	28, 1	2.580, 2.578	440, 521
11	2.449	7	2.448	223
17	2.383	14	2.382	313
10	2.360	8	2.360	512
7	2.223	2, 2	2.224, 2.212	621, 403
5	2.086	4	2.086	004
13	2.008	1, 11	2.006, 2.004	204, 551
1	1.965	2	1.967	641
2	1.938	2	1.934	224
11	1.868	13	1.868	731
14	1.825	19	1.824	800
9	1.812	8	1.811	404
3	1.777	1, 1, 1, 2	1.784, 1.782, 1.776, 1.770	334, 801, 623, 820
12	1.659	20	1.657	713
5	1.635	5	1.629	822
6	1.623	3	1.622	444
6	1.588	6	1.588	225
9	1.580	15	1.578	733
9	1.520	10, 6	1.520, 1.518	842, 405
7	1.467	10	1.467	554
6	1.452	6	1.452	771
6	1.443	1, 5, 3	1.443, 1.442, 1.438	932, 515, 10.0.1
3	1.344	3, 4	1.350, 1.342	824, 952
5	1.291	1, 1, 2, 8	1.292, 1.290, 1.289, 1.289	863, 880, 336, 10.4.2
2	1.265	3	1.265	971
4	1.204	3	1.204	774

* For the calculated pattern, only reflections with intensities ≥ 1 are given; ** for the unit-cell parameters calculated from single-crystal data; the strongest reflections are marked in bold type.

VariMAX microfocuss optics), 40 kV, 15 mA and an exposure time of 15 min. Angular resolution of the detector is 0.045 2 θ (pixel size = 0.1 mm). The data were integrated using the software

Table 3. Crystal data, data collection information and structure refinement details for axelite.

Crystal data	
Formula obtained from structure refinement	(Na _{0.88} Cu _{0.12})(Na _{0.97} Cu _{0.03})Na _{3.5} (Na _{0.95} □ _{0.05}) ₂ (Cu _{0.99} □ _{0.01})(Cu _{0.71} Na _{0.25} □ _{0.04}) _{0.5} (Cu _{0.97} □ _{0.03}) ₂ [(As _{0.87} P _{0.13} O ₄) ₂ [AsO ₄] ₂ Cl(F _{0.76} O _{0.24})
Formula weight	985.36
Unit cell dimensions (Å)	<i>a</i> = 14.5957(2), <i>c</i> = 8.34370(18)
Crystal system, space group, <i>Z</i>	Tetragonal; <i>P4bm</i> ; 4*
<i>V</i> (Å ³)	1777.51(6)
Absorption coefficient μ (mm ⁻¹)	11.407
<i>F</i> ₀₀₀	1847
Data collection	
Crystal size (mm)	0.03 × 0.05 × 0.06
Temperature (K)	293(2)
Diffractometer	Xcalibur S CCD
Radiation and wavelength (Å)	MoK α ; 0.71073
θ range for data collection (°) / Collection mode	2.79–28.26 / full sphere
Index ranges	–19 ≤ <i>h</i> ≤ 19, –19 ≤ <i>k</i> ≤ 19, –11 ≤ <i>l</i> ≤ 11
Reflections collected	29,213
Independent reflections	2330 (<i>R</i> _{int} = 0.0674)
Independent reflections with <i>I</i> > 2 σ (<i>I</i>)	2247
Data reduction	<i>CrysAlisPro</i> , v. 1.171.39.46 (Rigaku OD, 2018)
Absorption correction	Gaussian
Structure solution	Direct methods
Refinement	
Refinement method	Full-matrix least-squares on <i>F</i> ²
Number of refined parameters	175
Final <i>R</i> indices [<i>I</i> > 2 σ (<i>I</i>)]	<i>R</i> ₁ = 0.0450, <i>wR</i> ₂ = 0.0960
<i>R</i> indices (all data)	<i>R</i> ₁ = 0.0476, <i>wR</i> ₂ = 0.0972
GoF	1.163
Largest diff. peak and hole (e ⁻ /Å ³)	1.83 and –0.96

**Z* = 2 for the idealised formula with whole-number coefficients, Na₁₄Cu₇(AsO₄)₈F₂Cl₂.

package *Osc2Tab* (Britvin *et al.*, 2017). The tetragonal unit cell parameters refined from the powder data are: *a* = 14.604(2), *c* = 8.348(2) Å and *V* = 1780(1) Å³.

A single-crystal XRD study of axelite was carried out using an Xcalibur S diffractometer equipped with a CCD detector (MoK α radiation). A full sphere of three-dimensional data was collected. Intensity data were corrected for Lorentz and polarisation effects. The crystal structure of the mineral was solved by direct methods and refined using the *SHELX* software package (Sheldrick, 2015) to *R* = 0.0450 on the basis of 2247 independent reflections with *I* > 2 σ (*I*). Crystal data, data collection information and structure refinement details are given in Table 3, coordinates and equivalent displacement parameters of atoms in Table 4, selected interatomic distances in Table 5, and bond valence calculations in Table 6. The crystallographic information file has been deposited with the Principal Editor of *Mineralogical Magazine* and is available as Supplementary material (see below).

Discussion

No mineral or synthetic compound closely related to axelite is found in literature and databases: it represents a novel structure type. In addition, being a H-free mineral, axelite is distantly related, in both structural and chemical aspects, to lavendulan-like hydrous arsenates and phosphates [primarily Cl-bearing species mahnertite (Na,Ca,K)Cu₃(AsO₄)₂Cl·5H₂O (Pushcharovsky *et al.*, 2004), zdeněkite NaPbCu₅(AsO₄)₄Cl·5H₂O (Zubkova *et al.*, 2003), lavendulan NaCaCu₅(AsO₄)₄Cl·5H₂O and sampleite

Table 4. Coordinates and equivalent displacement parameters (U_{eq} , in Å²) of atoms, site multiplicities (Q) and site occupancies for axelite.

Site	Site occupancies	Q	x	y	z	U_{eq}
As(1)	As _{0.868(15)} P _{0.132(15)}	8	0.00716(7)	0.71732(8)	-0.00216(12)	0.0061(4)
As(2)	1	8	0.00536(7)	0.79284(7)	0.43897(12)	0.0091(3)
Cu(1)	0.988(10)	4	0.11684(11)	0.61684(11)	0.2859(4)	0.0133(7)
Cu(2)	0.712(17)	2	½	½	0.5725(7)	0.0081(13)
Na'	0.25*	2	½	½	0.485(8)	0.012(9)
Cu(3)	0.968(9)	8	0.39170(9)	0.61398(10)	0.1440(2)	0.0108(5)
Na(1)	Na _{0.879(18)} Cu _{0.121(18)}	4	0.1156(4)	0.3844(4)	0.2883(15)	0.048(3)
Na(2)	Na _{0.969(19)} Cu _{0.031(19)}	4	0.7530(3)	0.7470(3)	0.9824(9)	0.018(3)
Na(3)	1	4	0.2512(3)	0.7512(3)	0.4641(8)	0.0098(13)
Na(4)	1	4	0.8782(4)	0.6218(4)	0.6690(9)	0.0208(16)
Na(5)	1	2	½	0.0	0.9580(14)	0.021(2)
Na(6)	0.95*	8	0.8769(4)	0.8521(4)	0.7545(7)	0.0201(13)
Na(7)	1	4	0.1277(4)	0.6277(4)	0.6697(8)	0.0210(16)
Cl(1)	1	2	0.0	½	0.4915(9)	0.0194(12)
Cl(2)	1	2	½	½	-0.0561(8)	0.0160(11)
O(1)	1	8	0.5032(6)	0.8395(7)	0.8310(10)	0.022(2)
O(2)	1	8	0.0980(5)	0.7862(5)	0.0029(11)	0.0149(16)
O(3)	1	8	0.0110(6)	0.6442(6)	0.1518(12)	0.0183(18)
O(4)	1	8	-0.0902(5)	0.7770(5)	0.0148(11)	0.0171(18)
O(5)	1	8	-0.0932(6)	0.7390(6)	0.4563(11)	0.022(2)
O(6)	1	8	0.0954(6)	0.7216(5)	0.4292(11)	0.0147(17)
O(7)	1	8	0.0218(6)	0.8640(6)	0.5947(10)	0.0194(19)
O(8)	1	8	0.0041(5)	0.8606(6)	0.2720(10)	0.0159(17)
F	F _{0.76} O _{0.24} *	4	0.7537(5)	0.7463(5)	0.7243(14)	0.0195(19)

*Fixed on the last stage of the refinement for charge balance.

A small amount of Cu²⁺ could also be present as an admixture in the Na(3) site (possibly accompanied with a vacancy). In this case, the highest peak on the difference-Fourier synthesis (1.83e/Å³) with $x = 0.2556$, $y = 0.2444$ and $z = 0.2211$ could be considered as an additional ligand for Cu²⁺ in the Na(2) and Na(3) sites slightly occupied by O²⁻. Interatomic distances between this additional ligand and the Na(2) and Na(3) sites are ~2.00 and 2.03 Å.

Table 5. Selected interatomic distances (Å) in the structure of axelite.

As(1)–O(1)	1.621(9)	Cu(2)–O(7)	2.019(9) ×4	Na(2)–F	2.153(13)	Na(6)–O(7)	2.281(10)
As(1)–O(2)	1.665(7)	Cu(2)–Cl(2)	3.099(9)	Na(2)–O(2)	2.320(9) ×2	Na(6)–F	2.384(6)
As(1)–O(3)	1.671(10)			Na(2)–O(4)	2.346(9) ×2	Na(6)–O(4)	2.479(10)
As(1)–O(4)	1.673(8)	Cu(3)–O(4)	1.940(8)			Na(6)–O(7)	2.506(10)
		Cu(3)–O(2)	1.952(8)	Na(3)–F	2.172(14)	Na(6)–O(2)	2.565(10)
As(2)–O(5)	1.645(8)	Cu(3)–O(8)	1.980(8)	Na(3)–O(5)	2.277(9) ×2	Na(6)–O(5)	3.018(11)
As(2)–O(6)	1.678(8)	Cu(3)–O(8)	1.992(8)	Na(3)–O(6)	2.332(9) ×2	Na(6)–Cl(2)	3.223(7)
As(2)–O(7)	1.680(8)	Cu(3)–Cl(2)	2.838(4)				
As(2)–O(8)	1.708(8)			Na(4)–O(1)	2.340(10) ×2	Na(7)–O(1)	2.311(10) ×2
		Na'–O(7)	2.21(3) ×4	Na(4)–O(5)	2.500(10) ×2	Na(7)–O(6)	2.476(10) ×2
Cu(1)–O(3)	1.949(9) ×2	Na'–O(8)	2.70(4) ×4	Na(4)–F	2.611(12)	Na(7)–F	2.641(12)
Cu(1)–O(6)	1.966(8) ×2			Na(4)–Cl(1)	2.918(8)	Na(7)–Cl(1)	3.026(8)
Cu(1)–Cl(1)	2.960(5)	Na(1)–O(3)	2.210(11) ×2				
		Na(1)–O(5)	2.306(12) ×2	Na(5)–O(1)	2.572(11) ×4		
		Na(1)–Cl(1)	2.927(12)	Na(5)–O(3)	2.659(12) ×4		

NaCaCu₅(PO₄)₄Cl·5H₂O (Giester *et al.*, 2007)] and analogous natural and synthetic compounds (Kiriukhina *et al.*, 2022 and references therein). It is noteworthy, however, all these hydrous minerals of supergene origin differ strongly from axelite in unit-cell dimensions, powder XRD and the majority of physical properties.

In the axelite structure (Figs 3, 4, 5 and 6a), the important unit is the heteropolyhedral chain running along the c axis and built by clusters formed by CuO₄Cl square pyramids connected with AsO₄ tetrahedra. Topologically the same clusters were reported in lavendulan-type minerals and structurally related compounds (Giester *et al.*, 2007 and references therein) and are shown in Fig. 6b,c. The cluster in axelite consists of four Cu(3)O₄Cl pyramids linked to each other *via* common O–Cl edges (four O atoms and one common Cl atom) thus forming a [Cu₄O₁₂Cl] unit. Eight AsO₄ tetrahedra share vertices with this unit; four of them, As(2)O₄ tetrahedra, are further bound *via* common vertices

with the tetragonal base of the fifth Cu(2)O₄Cl square pyramid that shares a common Cl atom with the neighbouring [Cu₄O₁₂Cl] unit. Thus the heteropolyhedral chains (Fig. 3a) are formed. In contrast to lavendulan-type minerals and the majority of the structurally related compounds in which, topologically, the same clusters consisting of five tetragonal pyramids and eight T⁵⁺O₄ tetrahedra ($T = \text{As, P}$) are connected to form heteropolyhedral layers, in axelite the linkage of the fifth Cu(2)O₄Cl square pyramid to the neighbouring [Cu₄O₁₂Cl] unit *via* the common Cl vertex allows the heteropolyhedral chains to be considered as the main building block. Among lavendulan-like compounds, a similar linkage of the fifth tetragonal pyramid to the neighbouring cluster was found in Ba(VO)Cu₄(PO₄)₄ (tetragonal, $P4_21_2$, $a = 9.5598$, $c = 7.160$ Å: Meyer and Müller-Buschbaum, 1997) (Fig. 4c,d), synthetic phosphates isostructural with this compound A(TiO)Cu₄(PO₄)₄ ($A = \text{Ba, Sr and Pb}$) (Kimura *et al.*, 2016, 2018), and structurally close K(NbO)Cu₄(PO₄)₄ (tetragonal, $P4/nmm$,

Table 6. Bond valence calculations for axelite.

	As(1)	As(2)	Cu(1)	Cu(2)	Na'	Cu(3)	Na(1)	Na(2)	Na(3)	Na(4)	Na(5)	Na(6)	Na(7)	Σ
Cl(1)			0.07 ^{x2→}				0.12 ^{x2→}			0.13 ^{x2→}			0.09 ^{x2→}	0.82
Cl(2)				0.04		0.10 ^{x4→}						0.05 ^{x4→}		0.64
O(1)	1.44									0.22 ^{x2↓}	0.12 ^{x4↓}		0.23 ^{x2↓}	2.01
O(2)	1.27					0.46		0.23 ^{x2↓}				0.12		2.08
O(3)	1.25		0.47 ^{x2↓}				0.29 ^{x2↓}				0.10 ^{x4↓}			2.11
O(4)	1.25					0.47		0.21 ^{x2↓}				0.15		2.08
O(5)		1.41					0.23 ^{x2↓}		0.25 ^{x2↓}	0.15 ^{x2↓}		0.04		2.08
O(6)		1.28	0.45 ^{x2↓}						0.22 ^{x2↓}				0.16 ^{x2↓}	2.11
O(7)		1.27		0.28 ^{x4↓}	0.07 ^{x4↓}							0.24		2.00
												0.14		
O(8)		1.18			0.02 ^{x4↓}	0.42	0.41							2.03
F								0.28	0.26	0.08		0.14 ^{x2→}	0.07	0.97
Σ	5.21	5.14	1.91	1.16*	0.36*	1.86	1.16	1.16	1.20**	0.95	0.88	0.88	0.94	

Bond-valence parameters were taken from Gagné and Hawthorne (2015); for Cu–Cl, Na–Cl and Na–F the parameters were taken from Brese and O'Keeffe (1991). For (F,O) site parameters of F were used. Site occupancies (Table 4) were taken into account.

*The Cu(2) site could possibly accommodate a small amount of Na. The Na' site is located near Cu(2) [Cu(2)–Na' = 0.73(4) Å and this makes impossible their simultaneous filling] and could contain a small amount of Ca²⁺. **The Na(3) site could contain admixed Cu²⁺ with simultaneous presence of vacancy (see footnote of Table 4).

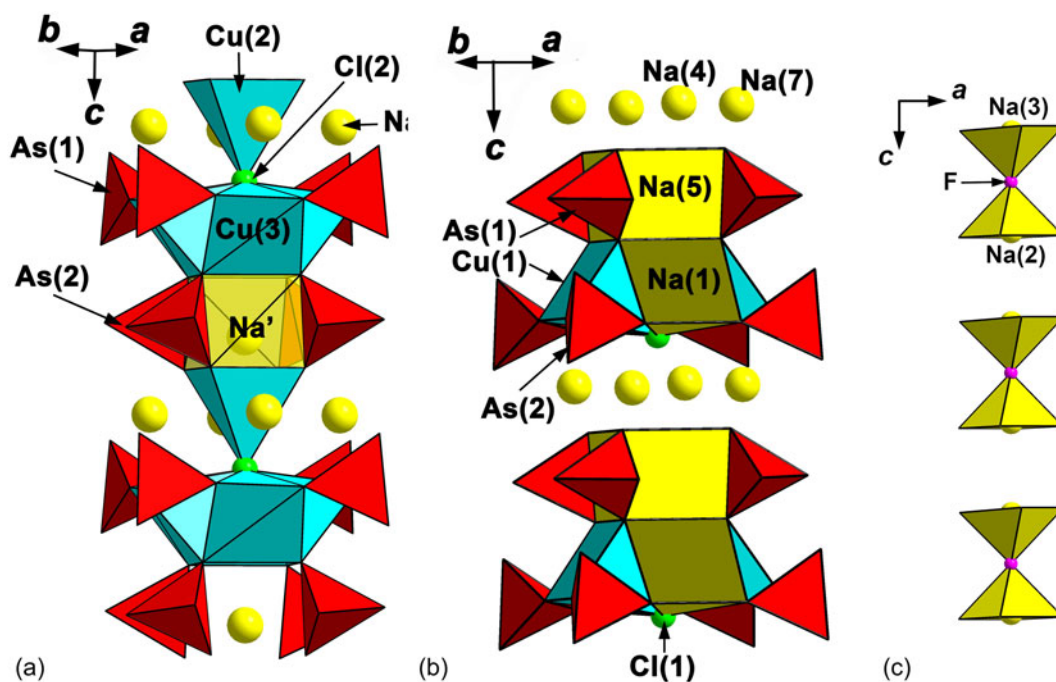


Fig. 3. Fragments of the crystal structure of axelite: (a) heteropolyhedral chain built by [Cu(3)₄O₁₂Cl] units, AsO₄ tetrahedra and Cu(2)O₄Cl square pyramids; an additional Na' site is shown, its coordination polyhedron is semi-transparent; (b) a fragment consisting of [Na₂Cu₂O₁₂Cl] clusters, AsO₄ tetrahedra and Na(5)O₈ cubes; (c) dimers built by Na(2) and Na(3) square pyramids.

$a = 9.6865$, $c = 7.1530$ Å; Kimura *et al.*, 2020). Adjacent chains in axelite are connected *via* common vertices of AsO₄ tetrahedra with Cu(1)₂O₈Cl dimers built by two Cu(1)-centred square pyramids with the common Cl vertex thus forming a heteropolyhedral pseudo-framework (Fig. 4a,b). All Cu²⁺ cations in axelite have, due to the Jahn-Teller effect, [4+1] coordination and centre tetragonal pyramids. In each of these polyhedra, the square base is built by O atoms with Cu–O distances lying in the range from 1.94 to 2.02 Å, whereas the apical ligand is a Cl atom and Cu–Cl distances vary from 2.84 to 3.10 Å (Table 5). For the Cu(1) and Cu(3) sites, occupancy factors (s.o.f.) are close to 1.0 (0.99 and 0.97, respectively), however the Cu(2) site is filled only to 71%. An additional Na' site with s.o.f. 0.25 is localised near Cu(2) from the difference-Fourier synthesis [Cu(2)–Na' = 0.73 Å

thus these positions cannot be filled simultaneously]. This site is located inside the chain, directly on its axis, between four As(2)O₄ tetrahedra and the [Cu₄O₁₂Cl] unit, and centres a slightly distorted cube Na'O₈, which shares four common edges with As(2)O₄ tetrahedra and four edges with Cu(3)O₄Cl pyramids. The Na(6) sites are also located inside the chain but around its axis, at the same height as the Cu(2)-centred pyramid (Fig. 3a). They centre seven-fold polyhedra Na(6)O₅FCl. The Na(1) site shows a distinct partial substitution of Na by Cu (Tables 4 and 6) and centres a square pyramid with four O atoms in the square base and Na(1)–O distances in the range from 2.21 to 2.30 Å and an elongated fifth bond Na(1)–Cl(1) = 2.93 Å. Two Na(1)O₄Cl pyramids share common O–Cl(1) edges with two Cu(1)O₄Cl pyramids thus forming topologically the same cluster [Na₂Cu₂O₁₂Cl]

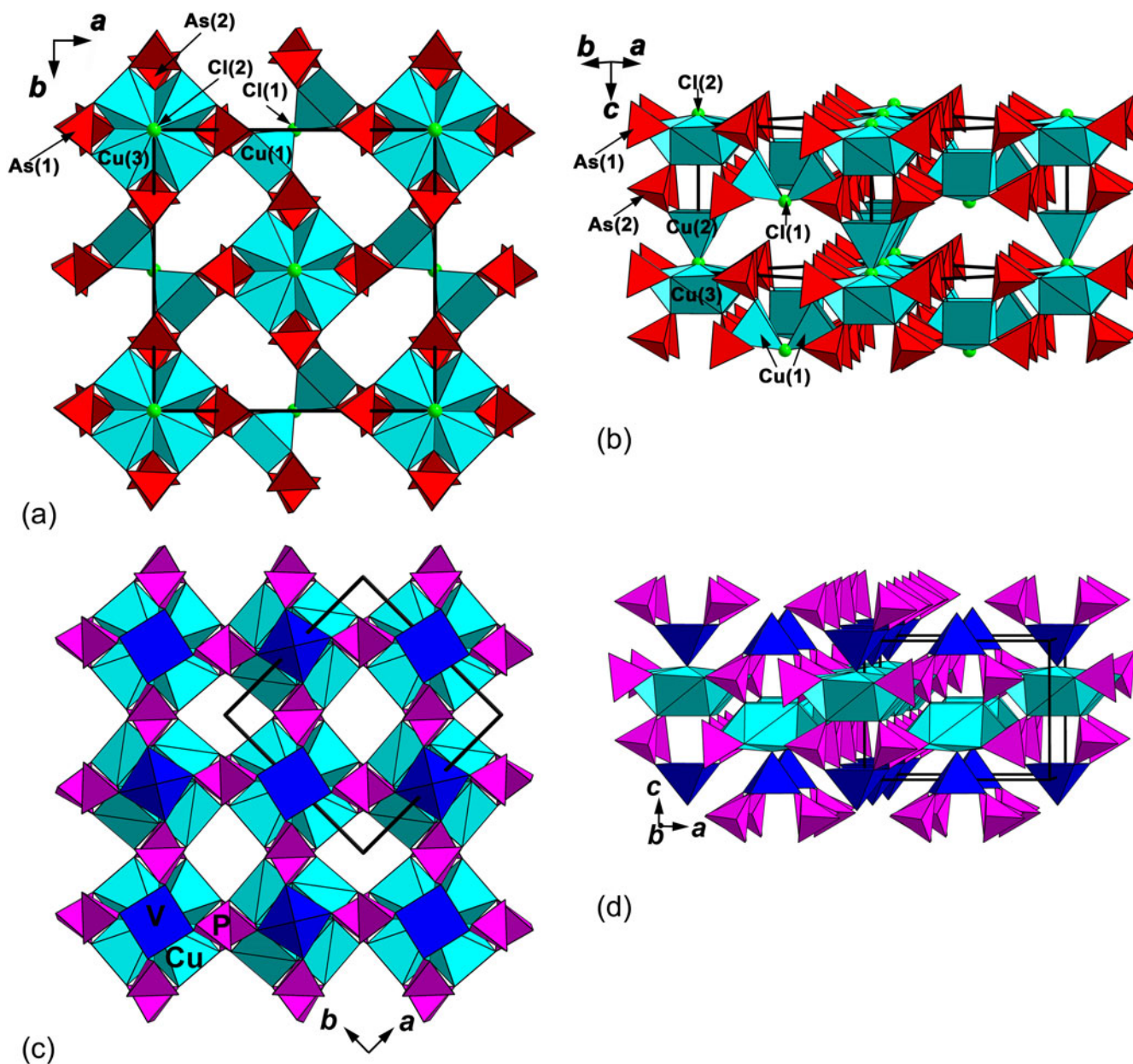


Fig. 4. Heteropolyhedral Cu–As–O–Cl pseudo-framework in the structure of axelite in two projections (a,b) and Cu–P–V–O pseudo-framework in $\text{Ba}(\text{VO})\text{Cu}_4(\text{PO}_4)_4$ (c,d, drawn after Meyer and Müller-Buschbaum, 1997). The unit cells are outlined.

as was determined for Cu(3)-centred polyhedron. Eight AsO_4 tetrahedra share vertices with this unit in the same way as described above for the heteropolyhedral chains. The Na(5) site centres a slightly distorted cube sharing four common edges with $\text{As}(1)\text{O}_4$ tetrahedra, two edges with two $\text{Cu}(1)\text{O}_4\text{Cl}$ pyramids and two edges with two $\text{Na}(1)\text{O}_4\text{Cl}$ pyramids. The position of Na(5)-centred cubes is similar with the location of Na^+ -centred cubes inside the above-described chains (Fig. 3a). Thus, interrupted heteropolyhedral chains topologically close to those described above and shown in Fig. 3a, however, do not contain additional Cu(2)-centred pyramids. The Na(4) and Na(7) sites centre distorted NaO_4FCl octahedra and are located inside these interrupted chains around their axes (Fig. 3b), similarly to Na(6) cations (Fig. 3a). The Na(2) and Na(3) sites are located in channels of the heteropolyhedral pseudo-framework and centre

square pyramids with four elongated Na–O bonds, forming the base of the pyramids, and one short Na–F bond (Table 5). Adjacent Na(2)- and Na(3)-centred pyramids share common F vertices to form dimers (Fig. 3c). The structures of axelite (tetragonal) and two distantly related hydrous copper chloro-arsenates lavendulan (monoclinic, pseudotetragonal: Giester *et al.*, 2007) and mahnertite (tetragonal: Pushcharovsky *et al.*, 2004) are compared in Fig. 6. In the layered structures of lavendulan (Fig. 6b), zdenekite, sampleite (Giester *et al.*, 2007), richelsdorffite $\text{Ca}_2\text{Cu}_5\text{SbCl}(\text{OH})_6(\text{AsO}_4)_4 \cdot 6\text{H}_2\text{O}$ (Süsse and Tillmann, 1987) and synthetic $\text{Na}_2\text{Li}_{0.75}(\text{Cs},\text{K})_{0.5}[\text{Cu}_5(\text{PO}_4)_4\text{Cl}] \cdot 3.5(\text{H}_2\text{O},\text{OH})$ (Kiriukhina *et al.*, 2022), $\text{Na}_5\text{ACu}_4(\text{AsO}_4)_4\text{Cl}_2$ ($A = \text{Rb}$ and Cs) (Hwu *et al.*, 2002), $\text{Na}_3\text{Cu}_5(\text{PO}_4)_4\text{F} \cdot 4\text{H}_2\text{O}$ (Yue *et al.*, 2018) and $\text{Sr}_2\text{Cu}_5(\text{PO}_4)_4\text{X}_2 \cdot 8\text{H}_2\text{O}$ ($X = \text{Cl}$ and, Br) (Qiu *et al.*, 2017), the neighbouring heteropolyhedral layers are shifted relative to each

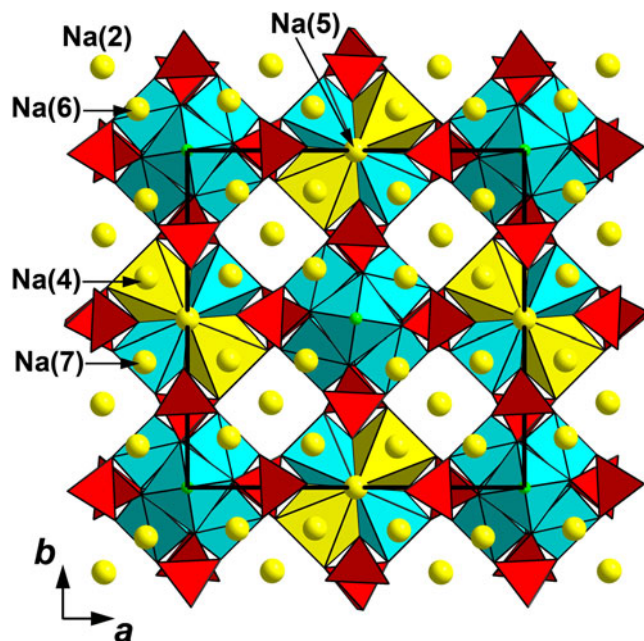


Fig. 5. The crystal structure of axelite in *ab* projection with Na(1) sites shown as polyhedra (yellow). The unit cell is outlined.

other. In mahnertite the neighbouring layers are connected with each other *via* the fifth vertices of the Cu-centred pyramids which do not belong to the $[\text{Cu}_4\text{O}_{12}\text{Cl}]$ clusters and their bases share all vertices with AsO_4 tetrahedra linked with the clusters forming a heteropolyhedral pseudo-framework (Fig. 6c). The same linkage of the heteropolyhedral layers was reported for the structure of a microporous potassium vanadyl phosphate analogue of mahnertite $\text{K}_{2.5}\text{Cu}_5\text{Cl}(\text{PO}_4)_4(\text{OH})_{0.5}(\text{VO}_2)\cdot\text{H}_2\text{O}$ (tetragonal: Yakubovich *et al.*, 2015). In andyrobtsite $\text{KCdCu}_5(\text{AsO}_4)_4(\text{AsO}_2(\text{OH})_2)\cdot 2\text{H}_2\text{O}$ (monoclinic: Cooper and Hawthorne, 2000) and calcioandyrobtsite-2O $\text{KCaCu}_5(\text{AsO}_4)_4(\text{AsO}_2(\text{OH})_2)\cdot 2\text{H}_2\text{O}$ (orthorhombic: Sarp and Černý, 2004), the layers are linked *via* additional As-centred tetrahedra. In axelite topologically close layers [in the case when Na(1)-centred tetragonal pyramids are also considered as the cluster-forming polyhedra] are linked *via* the tetragonal pyramids which do not participate in the clusters. However, in contrast with $\text{Ba}(\text{VO})\text{Cu}_4(\text{PO}_4)_4$ (Meyer and Müller-Buschbaum, 1997), phosphates $\text{A}(\text{TiO})\text{Cu}_4(\text{PO}_4)_4$ ($A = \text{Ba}, \text{Sr}$ and Pb) (Kimura *et al.*, 2016, 2018) and $\text{K}(\text{NbO})\text{Cu}_4(\text{PO}_4)_4$ (Kimura *et al.*, 2020), only one half of these pyramids are present in axelite (Fig. 4): the clusters with Na(1)-centred pyramids are not connected with the additional tetragonal pyramids.

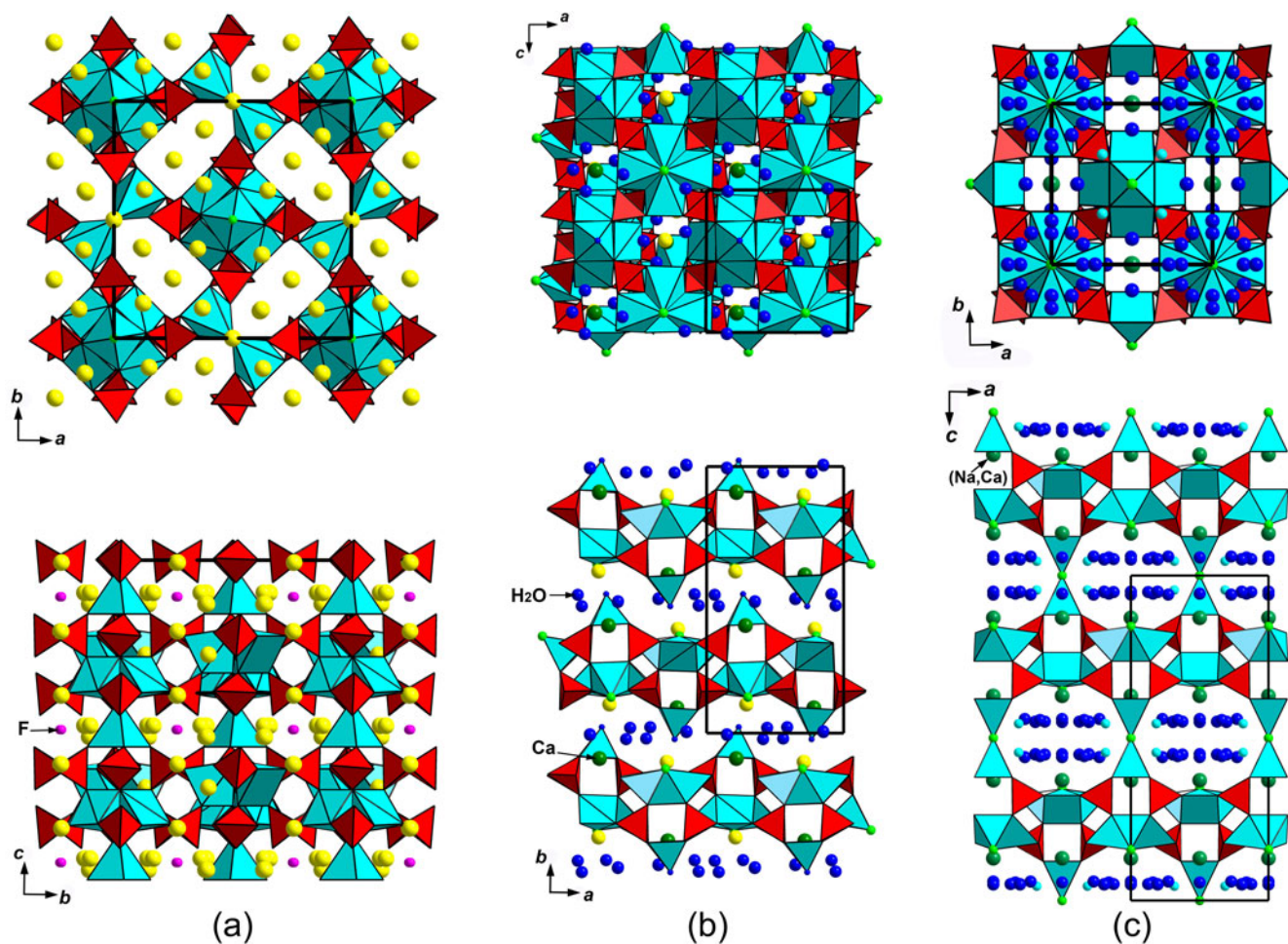


Fig. 6. Crystal structures of (a) axelite $\text{Na}_{14}\text{Cu}_7(\text{AsO}_4)_8\text{F}_2\text{Cl}_2$, (b) lavendulan $\text{NaCaCu}_5(\text{AsO}_4)_4\text{Cl}\cdot 5\text{H}_2\text{O}$ (drawn after Giester *et al.*, 2007), and (c) mahnertite $(\text{Na},\text{Ca})\text{Cu}_3(\text{AsO}_4)_2\text{Cl}\cdot 5\text{H}_2\text{O}$ (drawn after Pushcharovsky *et al.*, 2004), each in two projections. Cu-centred polyhedra are light blue (additional Cu sites in mahnertite are light-blue circles), AsO_4 tetrahedra are red, Cl atoms are light-green circles. The unit cells are outlined.

The crystal chemical formula of a crystal of axelite used for the structure determination (see Table 4) is $\text{Na}^{(1)}(\text{Na}_{0.88}\text{Cu}_{0.12})_2 \text{Na}^{(2)}(\text{Na}_{0.97}\text{Cu}_{0.03})_2 \text{Na}^{(3)}\text{Na}_2 \text{Na}^{(4)}\text{Na}_2 \text{Na}^{(5)}\text{Na} \text{Na}^{(6)}(\text{Na}_{0.95}\square_{0.05})_4 \text{Na}^{(7)}\text{Na}_2 \text{Cu}^{(1)}(\text{Cu}_{0.99}\square_{0.01})_2 \{\text{Na}'(\square_{0.75}\text{Na}_{0.25})\text{Cu}^{(2)}(\text{Cu}_{0.71}\square_{0.29})\} \text{Cu}^{(3)}(\text{Cu}_{0.97}\square_{0.03})_4 [\text{As}^{(1)}(\text{As}_{0.87}\text{P}_{0.13})\text{O}_4]_4 [\text{As}^{(2)}\text{AsO}_4]_4 \text{Cl}^{(1)}\text{Cl} \text{Cl}^{(2)}\text{Cl} \text{F}(\text{F}_{0.76}\text{O}_{0.24})_2 (Z = 2)$. This formally corresponds to the composition $\text{Na}_{14.75}\text{Cu}_{6.87}\text{P}_{0.52}\text{As}_{7.48}\text{O}_{32.48}\text{F}_{1.52}\text{Cl}_{2.00}$ that slightly differs, mainly in part of the Na:Cu ratio, from the empirical formula $\text{Na}_{14.37}\text{K}_{0.03}\text{Ca}_{0.01}\text{Mg}_{0.02}\text{Cu}_{6.63}\text{P}_{0.49}\text{V}_{0.03}\text{As}_{7.59}\text{S}_{0.01}\text{O}_{32.36}\text{F}_{1.63}\text{Cl}_{2.01}$ calculated from averaged electron microprobe data (Table 1). It is probably caused by slight ambiguity in the determination of content of several cationic sites: Na(1), Na(2) and, especially, adjacent and, therefore, partially occupied Na' and Cu(2). Thus we prefer (taking also into account that the Na' site is definitely vacancy-dominant) to use data from the electron microprobe which gives a whole-number coefficient of 14 for Na in the simplified formula of axelite: $\text{Na}_{14}\text{Cu}_7(\text{AsO}_4)_8\text{F}_2\text{Cl}_2 (Z = 2)$.

Acknowledgements. We thank Giuseppina Balassone, Oleg Siidra, two anonymous referees and Associate Editor Elena Zhitova for their valuable comments. The mineralogical and crystal chemical studies of axelite by IVP, NVZ and DYP were supported by the Russian Science Foundation, grant no. 19-17-00050. The technical support by the SPbSU X-Ray Diffraction Resource Center in the powder XRD study is acknowledged.

Supplementary material. To view supplementary material for this article, please visit <https://doi.org/10.1180/mgm.2022.120>

Competing interests. The authors declare none.

References

- Brese N.E. and O'Keeffe N.E. (1991) Bond-valence parameters for solids. *Acta Crystallographica*, **47**, 192–197.
- Britvin S.N., Dolivo-Dobrovolskiy D.V. and Krzhizhanovskaya M.G. (2017) Software for processing the X-ray powder diffraction data obtained from the curved image plate detector of Rigaku RAXIS Rapid II diffractometer. *Zapiski Rossiiskogo Mineralogicheskogo Obshchestva*, **146**, 104–107 [in Russian].
- Cooper M.A. and Hawthorne F.C. (2000) Highly undersaturated anions in the crystal structure of andyrobetsite – calcio-andyrobetsite, a doubly acid arsenate of the form $\text{K}(\text{Cd},\text{Ca})[\text{Cu}_2^{2+}(\text{AsO}_4)_4\{\text{As}(\text{OH})_2\text{O}_2\}](\text{H}_2\text{O})_2$. *The Canadian Mineralogist*, **38**, 817–830.
- Fedotov S.A. and Markhinin Y.K. (editors) (1983) *The Great Tolbachik Fissure Eruption*. Cambridge University Press, New York, 341 pp.
- Gagné O.C. and Hawthorne F.C. (2015) Comprehensive derivation of bond-valence parameters for ion pairs involving oxygen. *Acta Crystallographica*, **B71**, 562–578.
- Giester G., Kolitsch U., Leveret, P., Turner P. and Williams P.A. (2007) The crystal structures of lavendulan, sampleite, and a new polymorph of sampleite. *European Journal of Mineralogy*, **19**, 75–93.
- Hwu S.-J., Ulutagay-Kartin M., Clayhold J.A., Mackay R., Wardojo T.A., O'Connor C.J. and Krawiec M. (2002) A new class of hybrid materials via salt inclusion: novel copper(II) arsenates $\text{Na}_5\text{ACu}_4(\text{AsO}_4)_4\text{Cl}_2$ (A = Rb, Cs) composed of alternating covalent and ionic lattices. *Journal of the American Chemical Society*, **124**, 12404–12405.
- Kimura K., Sera M. and Kimura T. (2016) A^{2+} cation control of chiral domain formation in $\text{A}(\text{TiO})\text{Cu}_4(\text{PO}_4)_4$ (A = Ba, Sr). *Inorganic Chemistry*, **55**, 1002–1004.
- Kimura K., Toyoda M., Babkevich P., Yamauchi K., Sera M., Nassif V., Rønnow H.M. and Kimura T. (2018) A-cation control of magnetoelectric quadrupole order in $\text{A}(\text{TiO})\text{Cu}_4(\text{PO}_4)_4$ (A = Ba, Sr, and Pb). *Physical Review B*, **97**, 134418
- Kimura K., Urushihara D., Asaka T., Toyoda M., Miyake A., Tokunaga M. and Kimura T. (2020) Synthesis, structure, and anomalous magnetic ordering of the spin-½ coupled square tetramer system $\text{K}(\text{NbO})\text{Cu}_4(\text{PO}_4)_4$. *Inorganic Chemistry*, **59**, 10986–10995.

- Kiriukhina G., Yakubovich O., Shvanskaya L., Volkov A., Dimitrova O., Simonov S., Volkova O. and Vasiliev A. (2022) A novel mineral-like copper phosphate chloride with a disordered guest structure: crystal chemistry and magnetic properties. *Materials*, **15**, 1411
- Meyer S. and Müller-Buschbaum H. (1997) Cu_4O_{12} groups built of square planar CuO_4 polygons in the barium vanadyl oxocuprate(II) phosphate $\text{Ba}(\text{VO})\text{Cu}_4(\text{PO}_4)_4$. *Zeitschrift für Anorganische und Allgemeine Chemie*, **623**, 1693–1698.
- Pekov I.V., Zubkova N.V., Yapaskurt V.O., Belakovskiy D.I., Lykova I.S., Vigasina M.F., Sidorov E.G. and Pushcharovsky D.Yu. (2014a) New arsenate minerals from the Arsenatnaya fumarole, Tolbachik volcano, Kamchatka, Russia. I. Yurmarinite, $\text{Na}_7(\text{Fe}^{3+},\text{Mg},\text{Cu})_4(\text{AsO}_4)_6$. *Mineralogical Magazine*, **78**, 905–917.
- Pekov I.V., Zubkova N.V., Yapaskurt V.O., Belakovskiy D.I., Vigasina M.F., Sidorov E.G. and Pushcharovsky D.Yu. (2014b) New arsenate minerals from the Arsenatnaya fumarole, Tolbachik volcano, Kamchatka, Russia. II. Ericlaxmanite and kozyrevskite, two natural modifications of $\text{Cu}_4\text{O}(\text{AsO}_4)_2$. *Mineralogical Magazine*, **78**, 1527–1543.
- Pekov I.V., Zubkova N.V., Yapaskurt V.O., Belakovskiy D.I., Vigasina M.F., Sidorov E.G. and Pushcharovsky D.Yu. (2015a) New arsenate minerals from the Arsenatnaya fumarole, Tolbachik volcano, Kamchatka, Russia. III. Popovite, $\text{Cu}_5\text{O}_2(\text{AsO}_4)_2$. *Mineralogical Magazine*, **79**, 133–143.
- Pekov I.V., Zubkova N.V., Belakovskiy D.I., Yapaskurt V.O., Vigasina M.F., Sidorov E.G. and Pushcharovsky D.Yu. (2015b) New arsenate minerals from the Arsenatnaya fumarole, Tolbachik volcano, Kamchatka, Russia. IV. Shchurovskyite, $\text{K}_2\text{CaCu}_6\text{O}_2(\text{AsO}_4)_4$, and dmsokolovite, $\text{K}_3\text{Cu}_5\text{AlO}_2(\text{AsO}_4)_4$. *Mineralogical Magazine*, **79**, 1737–1753.
- Pekov I.V., Yapaskurt V.O., Britvin S.N., Zubkova N.V., Vigasina M.F. and Sidorov E.G. (2016a) New arsenate minerals from the Arsenatnaya fumarole, Tolbachik volcano, Kamchatka, Russia. V. Katiarsite, $\text{KTiO}(\text{AsO}_4)$. *Mineralogical Magazine*, **80**, 639–646.
- Pekov I.V., Zubkova N.V., Yapaskurt V.O., Polekhovskiy Yu.S., Vigasina M.F., Belakovskiy D.I., Britvin S.N., Sidorov E.G. and Pushcharovsky D.Yu. (2016b) New arsenate minerals from the Arsenatnaya fumarole, Tolbachik volcano, Kamchatka, Russia. VI. Melanarsite, $\text{K}_3\text{Cu}_7\text{Fe}^{3+}\text{O}_4(\text{AsO}_4)_4$. *Mineralogical Magazine*, **80**, 855–867.
- Pekov I.V., Yapaskurt V.O., Belakovskiy D.I., Vigasina M.F., Zubkova N.V. and Sidorov E.G. (2017a) New arsenate minerals from the Arsenatnaya fumarole, Tolbachik volcano, Kamchatka, Russia. VII. Pharmazincite, KZnAsO_4 . *Mineralogical Magazine*, **81**, 1001–1008.
- Pekov, I.V., Zubkova, N.V., Agakhanov, A.A., Yapaskurt, V.O., Belakovskiy, D.I., Britvin, S.N., Sidorov, E.G. and Pushcharovsky, D.Y. (2017b) Axelite, IMA 2017-015a. CNMNC Newsletter No. 38, August 2017, page 1038. *Mineralogical Magazine*, **81**, 1033–1038.
- Pekov I.V., Koshlyakova N.N., Zubkova N.V., Lykova I.S., Britvin S.N., Yapaskurt V.O., Agakhanov A.A., Shchupalkina N.V., Turchkova A.G. and Sidorov E.G. (2018a) Fumarolic arsenates – a special type of arsenic mineralization. *European Journal of Mineralogy*, **30**, 305–322.
- Pekov I.V., Zubkova N.V., Agakhanov A.A., Yapaskurt V.O., Chukanov N.V., Belakovskiy D.I., Sidorov E.G. and Pushcharovsky D.Yu. (2018b) New arsenate minerals from the Arsenatnaya fumarole, Tolbachik volcano, Kamchatka, Russia. VIII. Arsenowagnerite, $\text{Mg}_2(\text{AsO}_4)\text{F}$. *Mineralogical Magazine*, **82**, 877–888.
- Pekov I.V., Zubkova N.V., Agakhanov A.A., Belakovskiy D.I., Vigasina M.F., Yapaskurt V.O., Sidorov E.G., Britvin S.N. and Pushcharovsky D.Y. (2019a) New arsenate minerals from the Arsenatnaya fumarole, Tolbachik volcano, Kamchatka, Russia. IX. Arsenatrotitanite, $\text{NaTiO}(\text{AsO}_4)$. *Mineralogical Magazine*, **83**, 453–458.
- Pekov I.V., Zubkova N.V., Agakhanov A.A., Ksenofontov D.A., Pautov L.A., Sidorov E.G., Britvin S.N., Vigasina M.F. and Pushcharovsky D.Yu. (2019b) New arsenate minerals from the Arsenatnaya fumarole, Tolbachik volcano, Kamchatka, Russia. X. Edtollite, $\text{K}_2\text{NaCu}_5\text{Fe}^{3+}\text{O}_2(\text{AsO}_4)_4$, and alu-moedtollite, $\text{K}_2\text{NaCu}_5\text{AlO}_2(\text{AsO}_4)_4$. *Mineralogical Magazine*, **83**, 485–495.
- Pekov I.V., Lykova I.S., Yapaskurt V.O., Belakovskiy D.I., Turchkova A.G., Britvin S.N., Sidorov E.G. and Scheidl K.S. (2019c) New arsenate minerals from the Arsenatnaya fumarole, Tolbachik volcano, Kamchatka, Russia. XI. Anatolyite, $\text{Na}_6(\text{Ca},\text{Na})(\text{Mg},\text{Fe}^{3+})_3\text{Al}(\text{AsO}_4)_6$. *Mineralogical Magazine*, **83**, 633–638.

- Pekov I.V., Lykova I.S., Agakhanov A.A., Belakovskiy D.I., Vigasina M.F., Britvin S.N., Turchkova A.G., Sidorov E.G. and Scheidl K.S. (2019d) New arsenate minerals from the Arsenatnaya fumarole, Tolbachik volcano, Kamchatka, Russia. XII. Zubkovaite, $\text{Ca}_3\text{Cu}_3(\text{AsO}_4)_4$. *Mineralogical Magazine*, **83**, 879–886.
- Pekov I.V., Zubkova N.V., Koshlyakova N.N., Agakhanov A.A., Belakovskiy D.I., Vigasina M.F., Yapaskurt V.O., Britvin S.N., Turchkova A.G., Sidorov E.G. and Pushcharovsky D.Y. (2020a) New arsenate minerals from the Arsenatnaya fumarole, Tolbachik volcano, Kamchatka, Russia. XIII. Pansnerite, $\text{K}_3\text{Na}_3\text{Fe}_6^{3+}(\text{AsO}_4)_8$. *Mineralogical Magazine*, **84**, 143–151.
- Pekov I.V., Koshlyakova N.N., Agakhanov A.A., Zubkova N.V., Belakovskiy D.I., Vigasina M.F., Turchkova A.G., Sidorov E.G. and Pushcharovsky D.Yu. (2020b) New arsenate minerals from the Arsenatnaya fumarole, Tolbachik volcano, Kamchatka, Russia. XIV. Badalovite, $\text{NaNaMg}(\text{MgFe}^{3+})(\text{AsO}_4)_3$, a member of the alluaudite group. *Mineralogical Magazine*, **84**, 616–622.
- Pekov I.V., Agakhanov A.A., Zubkova N.V., Koshlyakova N.V., Shchipalkina N.V., Sandalov F.D., Yapaskurt V.O., Turchkova A.G. and Sidorov E.G. (2020c) Oxidizing-type fumaroles of the Tolbachik Volcano, a mineralogical and geochemical unique. *Russian Geology and Geophysics*, **61**, 675–688.
- Pekov I.V., Koshlyakova N.N., Agakhanov A.A., Zubkova N.V., Belakovskiy D.I., Vigasina M.F., Turchkova A.G., Sidorov E.G. and Pushcharovsky D.Yu. (2021a) New arsenate minerals from the Arsenatnaya fumarole, Tolbachik volcano, Kamchatka, Russia. XV. Calciojohillerite, $\text{NaCaMgMg}_2(\text{AsO}_4)_3$, a member of the alluaudite group. *Mineralogical Magazine*, **85**, 215–223.
- Pekov I.V., Zubkova N.V., Agakhanov A.A., Yapaskurt V.O., Belakovskiy D.I., Vigasina M.F., Britvin S.N., Turchkova A.G., Sidorov E.G. and Pushcharovsky D.Yu. (2021b) New arsenate minerals from the Arsenatnaya fumarole, Tolbachik volcano, Kamchatka, Russia. XVI. Yurgensonite, $\text{K}_2\text{SnTiO}_2(\text{AsO}_4)_2$, the first natural tin arsenate, and the katiarsite–yurgensonite isomorphous series. *Mineralogical Magazine*, **85**, 698–707.
- Pekov I.V., Koshlyakova N.N., Belakovskiy D.I., Vigasina M.F., Zubkova N.V., Agakhanov A.A., Britvin S.N., Sidorov E.G. and Pushcharovsky D.Yu. (2022a) New arsenate minerals from the Arsenatnaya fumarole, Tolbachik volcano, Kamchatka, Russia. XVII. Paraberzeliite, $\text{NaCaCaMg}_2(\text{AsO}_4)_3$, an alluaudite-group member dimorphous with berzeliite. *Mineralogical Magazine*, **86**, 103–111.
- Pekov I.V., Koshlyakova N.N., Belakovskiy D.I., Vigasina M.F., Zubkova N.V., Agakhanov A.A., Britvin S.N., Sidorov E.G. and Pushcharovsky D.Yu. (2022b) New arsenate minerals from the Arsenatnaya fumarole, Tolbachik volcano, Kamchatka, Russia. XVIII. Khrenovite, $\text{Na}_3\text{Fe}_3^{3+}(\text{AsO}_4)_3$, the member with the highest sodium in the alluaudite supergroup. *Mineralogical Magazine*, **86**, <https://doi.org/10.1180/mgm.2022.64>
- Pushcharovsky D.Yu., Zubkova N.V., Teat S.J., MacLean E.J. and Sarp H. (2004) Crystal structure of mahnertite. *European Journal of Mineralogy*, **16**, 687–692.
- Qiu C.Q., He Z.Z., Cui M.Y., Chen S.H. and Tang Y. (2017) Synthesis, structure and magnetic properties of new layered phosphate halides $\text{Sr}_2\text{Cu}_5(\text{PO}_4)_4\text{X}_2 \cdot 8\text{H}_2\text{O}$ (X = Cl, Br) with a crown-like building unit. *Dalton Transactions*, **46**, 4461–4466.
- Rigaku OD (2018) *CrysAlisPro Software System*, v. 1.171.39.46. Rigaku Corporation, Oxford, UK.
- Sarp H. and Černý R. (2004) Calcio-andyrobertsite-2O, $\text{KCaCu}_5(\text{AsO}_4)_4[\text{AsO}_2(\text{OH})_2] \cdot 2\text{H}_2\text{O}$: its description, crystal structure and relation with calcio-andyrobertsite-1M. *European Journal of Mineralogy*, **16**, 163–169.
- Shchipalkina N.V., Pekov I.V., Koshlyakova N.N., Britvin S.N., Zubkova N.V., Varlamov D.A. and Sidorov E.G. (2020) Unusual silicate mineralization in fumarolic sublimates of the Tolbachik volcano, Kamchatka, Russia – Part 1: Neso-, cyclo-, ino- and phyllosilicates. *European Journal of Mineralogy*, **32**, 101–119.
- Sheldrick G.M. (2015) Crystal structure refinement with SHELXL. *Acta Crystallographica*, **C71**, 3–8.
- Süsse P. and Tillmann B. (1987) The crystal structure of the new mineral richelsdorffite, $\text{Ca}_2\text{Cu}_5\text{Sb}(\text{Cl}/(\text{OH})_6)/(\text{AsO}_4)_4 \cdot 6\text{H}_2\text{O}$. *Zeitschrift für Kristallographie*, **179**, 323–334.
- Yakubovich O.V., Steele I.M., Kiriukhina G.V. and Dimitrova O.V. (2015) A microporous potassium vanadyl phosphate analogue of mahnertite: hydrothermal synthesis and crystal structure. *Zeitschrift für Kristallographie*, **230**, 337–344.
- Yue X., Ouyang Z., Cui M., Yin L., Xiao G., Wang Z., Liu J., Wang J., Xia Z., Huang X. and He Z. (2018) Syntheses, structure, and 2/5 magnetization plateau of a 2D layered fluorophosphate $\text{Na}_3\text{Cu}_5(\text{PO}_4)_4\text{F} \cdot 4\text{H}_2\text{O}$. *Inorganic Chemistry*, **57**, 3151–3157.
- Zubkova N.V., Pushcharovsky D.Y., Sarp H., Teat S.J. and MacLean E.J. (2003) Crystal structure of zdeněkite $\text{NaPbCu}_5(\text{AsO}_4)_4\text{Cl} \cdot 5\text{H}_2\text{O}$. *Crystallography Reports*, **48**, 939–943.